

# Production of Manganese-Zinc Ferrite Cores for Electronic Applications

Saw Mya Ni, and Kay Thi Lwin

**Abstract**—Ceramic ferrites are magnetic materials composed of selected oxides with iron oxides. The most common commercial soft magnetic materials are spinel ferrites, Mn-Zn and Ni-Zn ferrites having general structure  $AB_2O_4$ . The Manganese-Zinc ferrite is preferred for lower frequency applications less than 2 MHz where as Ni-Zn ferrite is preferred for higher frequency applications generally for power transformers, power inductors and general power applications. The microstructure and properties of ceramic ferrites depend critically upon the processing conditions.

The physical properties and sintering characteristics of  $(Mn_{(1-x)}Zn_x)Fe_2O_4$  have been carried out for equimolar composition,  $x = 0.5$ , at three sintering conditions; three sintering temperatures (1100, 1200 & 1300 °C) and three sintering times (1 hr, 2 hr & 3 hr). The X-ray diffraction analysis and Scanning Electron Microscopy were used for phase identification of Manganese Zinc Ferrites. The physical properties, density and shrinkage of the sample pellets have been studied by dimensional method and porosity by boiling water method.

**Keywords**—Powder Metallurgy, Manganese Zinc ferrite,  $(Mn_{(1-x)}Zn_x)Fe_2O_4$ .

## I. INTRODUCTION

TODAY, magnetic materials are found in numerous products around us- home appliances, electronic products, automobiles, communication equipments and data processing devices and equipments. These materials have now become a vital part of everyday life in modern industries. The magnetic materials used in early applications were metallic magnetic materials. But for frequencies exceeding MHz, metals and alloys are generally not suitable as soft magnets, as the eddy current losses are very high. The development of ferrites since 1946 reported that electrical resistivities of ferrites over a million times those of metals has an enormous impact in the application of magnetic materials particularly at high frequencies. Ferrites are used today in radio and television, microwave and satellite communication, bubble devices, audio, video and digital recording and as permanent magnets [1].

Saw Mya Ni is with Metallurgical Research and Development Center, Nay Pyi Taw, Myanmar (e-mail: arsaw2006@gmail.com).

Kay Thi Lwin, Pro- Rector, is with Technological University (TU) Thanlyin (e-mail: dr.ktlwin@gmail.com).

## II. EXPERIMENTAL PROCEDURE

The experimental procedure of Mn-Zn ferrite is shown with the schematic flow diagram as follows:

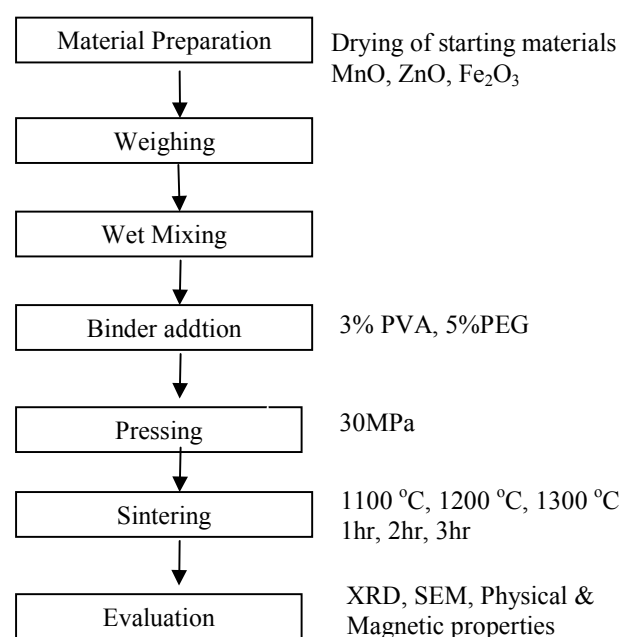


Fig. 1 Flow Diagram of Experimental Procedure

### Raw Materials Preparation

Manganese dioxide (MnO<sub>2</sub>), zinc oxide (ZnO) and ferric oxide (Fe<sub>2</sub>O<sub>3</sub>) were used as raw materials for production of Mn-Zn ferrite. The starting powers were technical grade of MnO<sub>2</sub>, ZnO and Fe<sub>2</sub>O<sub>3</sub> were 93.22%, 84.54%, and 80.33%. MnO<sub>2</sub> is reduced to MnO because manganese oxide (MnO) is not easily available in local market. MnO<sub>2</sub> (-270#) mixed with high quality coke (-48+ 65#) under reducing atmosphere.

Powder metallurgy method was used for production of Mn-Zn ferrite. The raw materials (MnO, ZnO, Fe<sub>2</sub>O<sub>3</sub>) were dried and weighed in stoichiometric ratio and then wet mixed in acetone medium for 1-2 hr to obtain thorough and homogeneous mixing.

3% PVA solution was added as a binder for improving compaction to the mixed powder and 5% PEG solution was added as a lubricant to prevent powders and die friction.

The mixed powder was palletized at 30 MPa pressure by hydraulic press machine and sintered in a high temperature

muffle furnace at three different sintering temperature of 1100°C, 1200°C and 1300°C and three sintering time 1hr, 2hr and 3hr respectively in order to achieve desirable physical properties and low porosity.

The sintered pellets were characterized by X- ray diffraction analysis and scanning electron microscopy for phase identification. The physical properties, the density and shrinkage were measured by dimensional method. The porosity was measured by boiling water method.

The electrical and magnetic properties; resistivity, relative permeability, magnetization, coercive force, remanence, magnetic flux density, magnetic field intensity and B-H characteristics were also measured.

### III. RESULTS AND DISCUSSION

X-ray diffraction analysis was used for characterization of phases. MnO phase was confirmed by X- ray diffraction analysis as shown in Fig. 2.

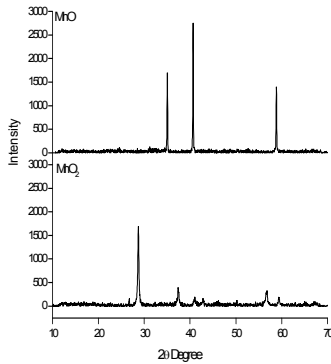


Fig. 2 XRD Pattern of MnO Compared with that of MnO<sub>2</sub> Powder Pattern

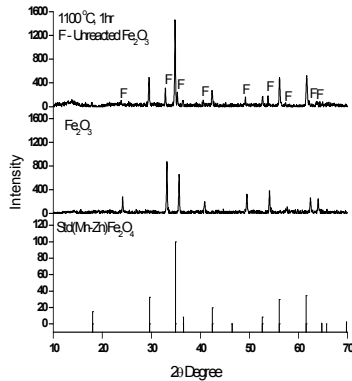


Fig. 3 XRD Pattern of Mn-Zn Ferrite Sintered at 1100°C for 1hr Compared with that of Standard JCPDF Data and Starting Powder Pattern

The following graphs are the XRD patterns of manganese zinc ferrite at different sintering times and temperatures. Fig. 3 shows X- ray diffraction analysis of Mn-Zn ferrite sintered at 1100°C for 1hr. Unreacted Fe<sub>2</sub>O<sub>3</sub> phases were observed at that

sintering condition showing this sintering temperature and time is not sufficient.

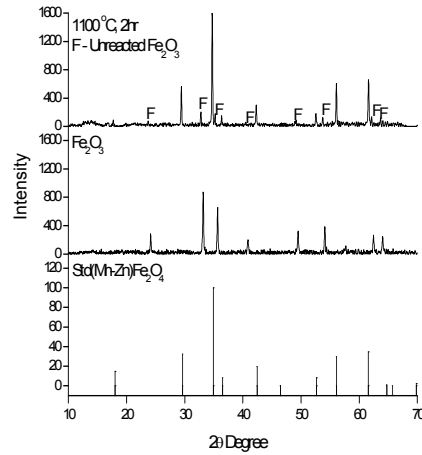


Fig. 4 XRD Pattern of Mn-Zn Ferrite Sintered at 1100° C for 2hr Compared with that of Standard JCPDF data and Starting Powder Pattern

Fig. 4 shows X- ray diffraction analysis of Mn-Zn ferrite sintered at 1100°C for 2hr. At this sintering temperature and time, unreacted Fe<sub>2</sub>O<sub>3</sub> phases were also observed. This shows that the sintering 1100°C and sintering time 2hrs was also not sufficient.

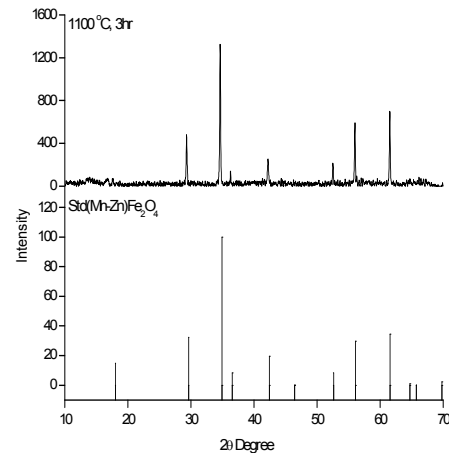


Fig. 5 XRD Pattern of Manganese Zinc Ferrite Sintered at 1100° C for 3hr Compared with that of Standard JCPDF data

Fig. 5 shows X-ray diffraction analysis of Mn-Zn ferrite sintered at 1100°C for 3hr. At this sintering temperature and sintering time, all the starting powders were completely reacted and spinel phases formation was confirmed.

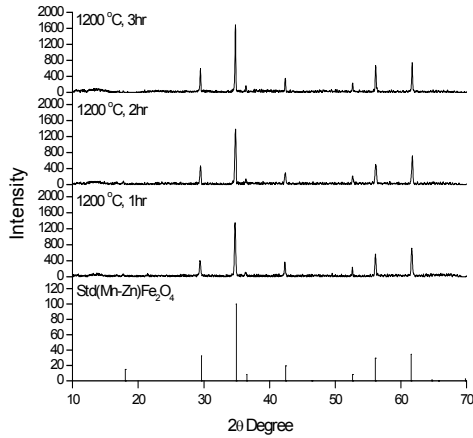


Fig. 6 XRD Pattern of Mn-Zn Ferrite Sintered at 1200°C for 1hr, 2hr & 3hr Compared with that of Standard JCPDF Data

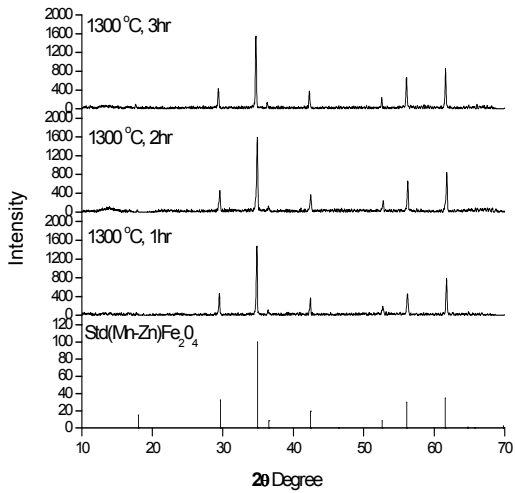


Fig. 7 XRD Pattern of Mn-Zn Ferrite Sintered at 1300° C for 1hr, 2hr & 3hr Compared with that of Standard JCPDF Data

Fig. 6 shows XRD pattern of manganese zinc ferrite sintered at constant temperature 1200°C by varying the sintering time for 1hr, 2hr and 3hr. At this temperature, spinel phases were confirmed for all the sintering time.

Fig. 7 shows XRD pattern of Mn-Zn ferrite sintered at constant temperature, 1300°C by varying sintering time for 1hr, 2hr and 3hr. The optimum sintering condition for Mn-Zn ferrite was observed at 1300°C for 3hr from the nature of the peak of X- Ray pattern.

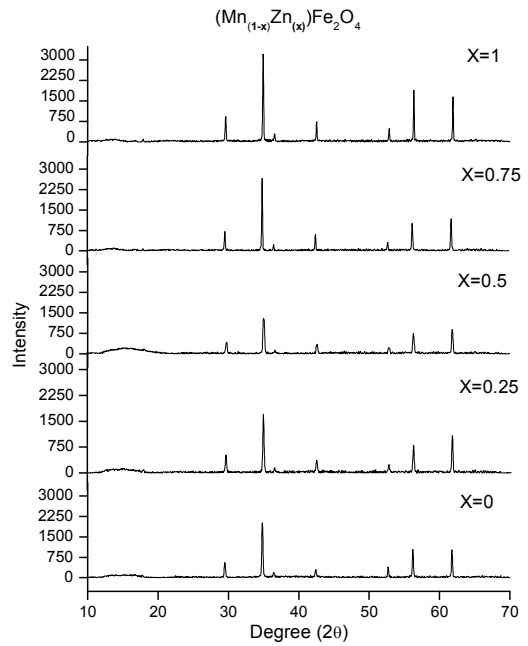


Fig. 8 Composite XRD Pattern of Mn-Zn Ferrite Sintered at Optimum Sintering Condition of 1300°C for 3 hr

Fig. 8 shows the composite XRD pattern of  $(Mn_{(1-x)}Zn_{(x)})Fe_2O_4$  for x = 0.5 composition at optimum sintering condition of 1300°C and sintering time 3hr. The ferrite pattern of Mn-Zn ferrite indicates the consistency with that of pure end member Mn ferrite and Zn ferrite spinels.

### Physical Properties

The results of the measurement of physical properties of Mn-Zn ferrite are presented in Figs. 9 to 12.

The graphs shown in Figure indicate the increasing of the density and shrinkage of the sintered pellets with increasing of the sintering conditions; times and temperatures.

But the porosity decreases as the sintering condition increases as shown in Fig. 12. All these graphs confirm that the physical properties increase with increasing of the sintering time and temperature.

The maximum sintering temperature of 1300°C and 3hr sintering time gives the 94% of theoretical density for  $(Mn_{(1-x)}Zn_{(x)})Fe_2O_4$ , x = 0.5.

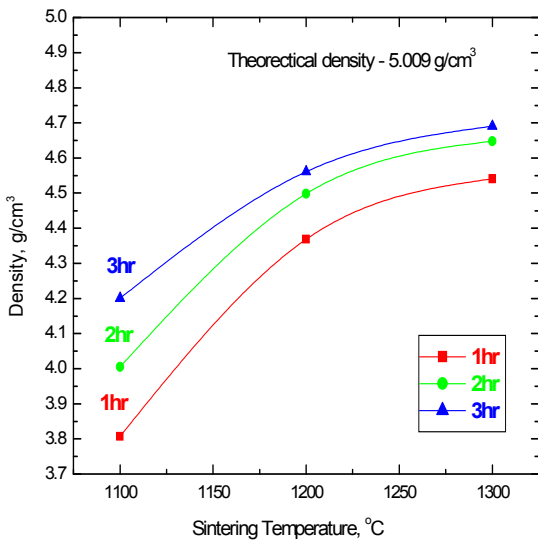


Fig. 9 Variation of Density with Different Sintering Condition for Mn-Zn Ferrite

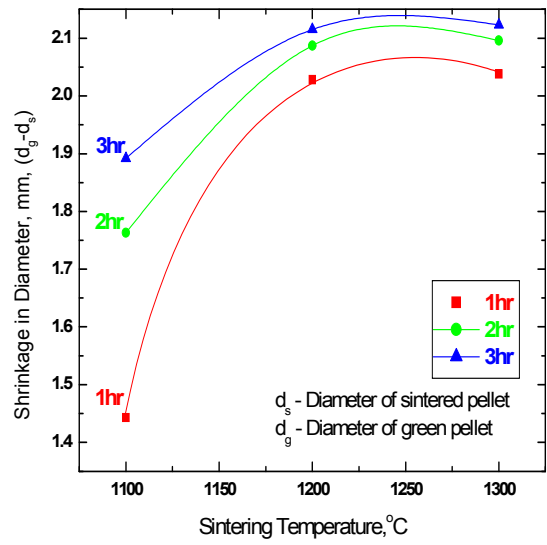


Fig. 11 Variation of Shrinkage in Thickness of Sintered Pellets at Different Sintering Condition

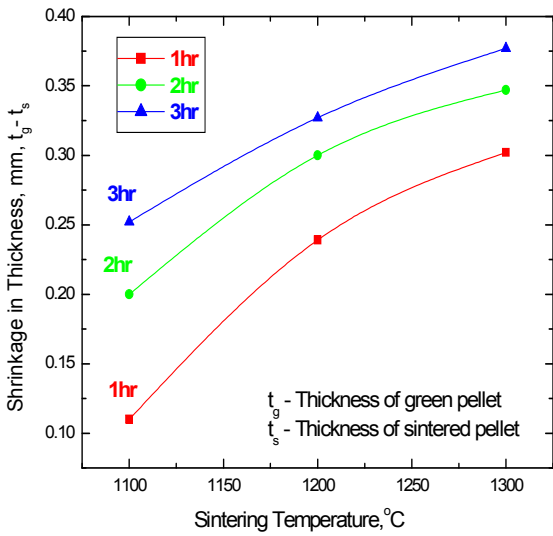


Fig. 10 Variation of Shrinkage in Diameter of Sintered Pellet at Different Sintering Condition

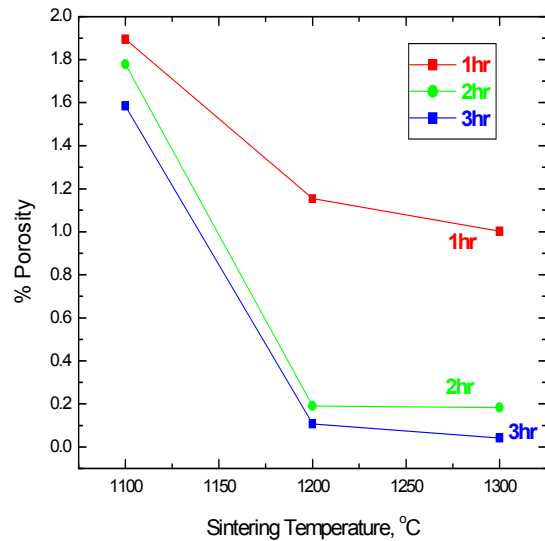


Fig. 12 Variation of Porosity with Different Condition for Mn-Zn Ferrite

### Spinel Phase Identification by Scanning Electron Microscopy

The scanning electron micrographs of manganese zinc ferrite were given in following figures.

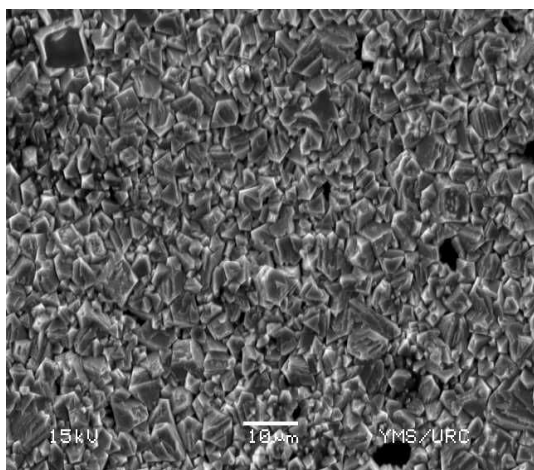


Fig. 13 SEM Micrograph of Mn-Zn Ferrite Sintered at 1200°C & 3hr with 10µ Scale

Fig. 13 shows scanning electron micrograph of manganese zinc ferrite sintered at 1200°C & 3hr with 10µ scale. Some pores can be seen this condition. The average grain size is 3.2µm.

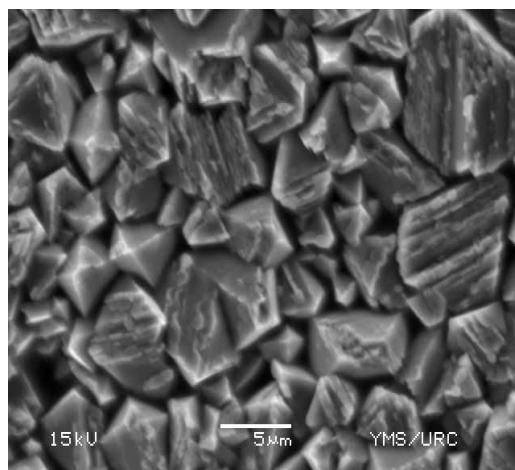


Fig. 15 SEM Micrograph of Mn-Zn Ferrite Sintered at 1250°C & 2hr with 5µ Scale

Fig. 15 shows scanning electron micrograph of manganese zinc ferrite sintered at 1250°C and 2hrs with 5µ scale just to enlarge the surface morphology.

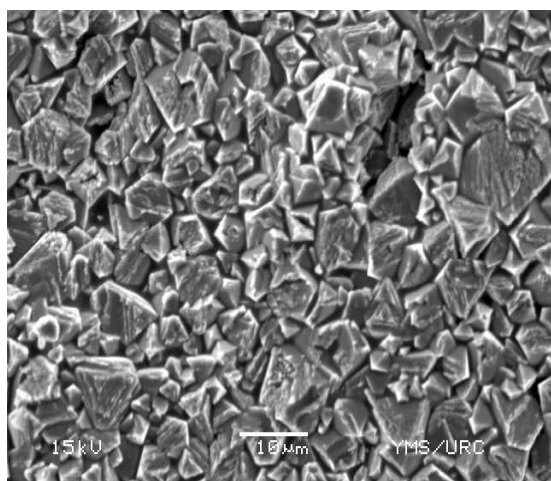


Fig. 14 SEM Micrograph of Mn-Zn Ferrite Sintered at 1250°C & 2hr with 10µ Scale

Fig. 14 shows scanning electron micrograph of manganese zinc ferrite sintered at 1250°C and 2hrs with 10µ scale. The average grain size is 4µm. Porosity decreases with increasing sintering time and temperature. The average grain size is 4µm.

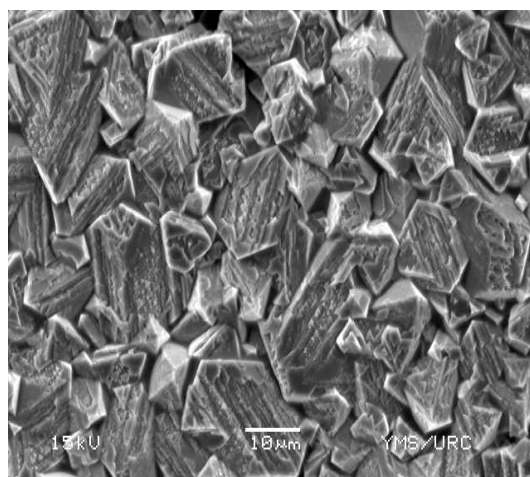


Fig. 16 SEM Micrograph of Mn-Zn Ferrite Sintered at 1300°C & 3hr with 10µ Scale

Fig. 16 shows scanning electron micrograph of manganese zinc ferrite sintered at 1300°C and 3hrs with 10µ scale. Average grain size is 6.9µm. By increasing sintering time and temperature, grain growth increases and the average grain size increases from 3.2µm in Fig. 13 to 6.9µm in Fig. 16.

**Magnetic Properties**

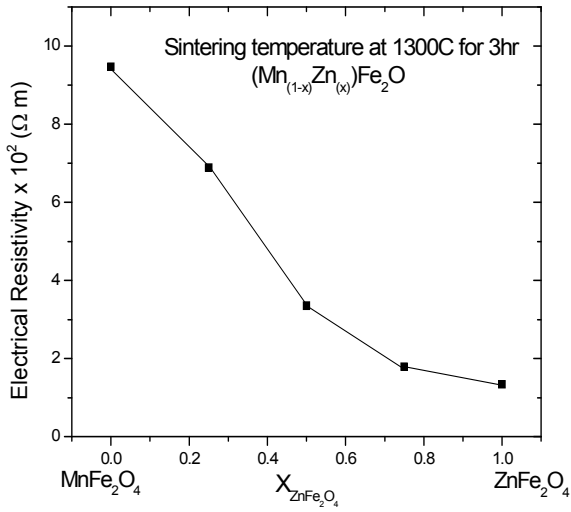


Fig. 17 The Variation of Electrical Resistivities of Mn-Zn Ferrite Depending on the Zn Addition

The variation of the electrical resistivity ( $\rho$ ) with increasing the composition of zinc ferrite, at room temperature, is represented in Fig. 17. It is obvious that the electrical resistivity is decreased rapidly by adding zinc ferrite.

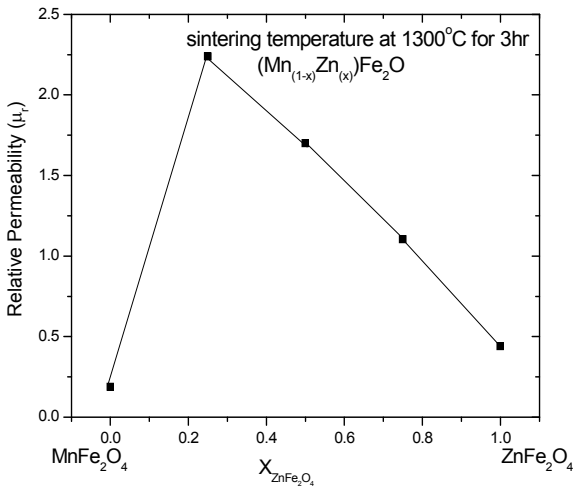


Fig. 18 Variation in Relative Permeability with Different Composition for Mn-Zn Ferrite Spinel

The composition dependence of the relative permeability at room temperature is represented in Fig. 18. Maximum relative permeability of  $(Mn_{(1-x)}Zn_x)Fe_2O_4$  was observed at  $ZnFe_2O_4$  composition 0.25.

The typical hysteresis loop of Mn-Zn ferrite using the measured data with oscilloscope is presented in Fig. 19. The magnetic properties of manganese zinc ferrite was observed high permeability, small coercive field, small remanence, small hysteresis loop, rapid response to high-frequency magnetic fields and low electrical resistivity.

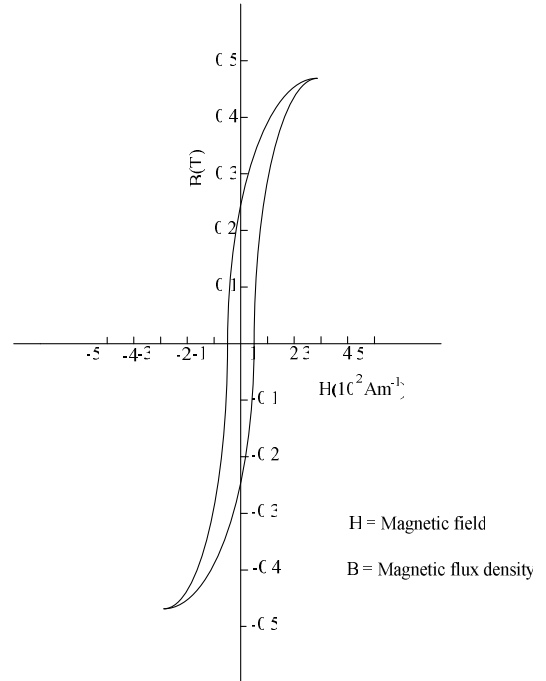


Fig. 19 Typical Hysteresis Loop of Mn-Zn Ferrite

**IV. CONCLUSION**

The sintering characteristics, physical properties, X-ray diffraction analysis and scanning electron microscopy as phase characterization techniques were studied. The fabrication of Mn-Zn ferrites  $(Mn_{(1-x)}Zn_x)Fe_2O_4$  have been studied at different sintering conditions. The optimum sintering condition was obtained at 1300°C and 3h. The density and shrinkage of the sintered pellets are increased with the increasing of sintering time and temperature. Maximum relative permeability of  $(Mn_{(1-x)}Zn_x)Fe_2O_4$  was observed at  $ZnFe_2O_4$  composition 0.25. The porosity was decreased with increasing of sintering time and temperature. The electrical resistivity of  $MnFe_2O_4$  is decreased rapidly by adding zinc ferrite. The magnetic properties of  $(Mn-Zn) Fe_2O_4$  are more or less in the range of standard value. The nature of the B-H curve also agrees with the nature of the standard B-H characteristic of  $(Mn-Zn)Fe_2O_4$ .

**REFERENCES**

- [1] Heck, C. 1974. Magnetic Materials and their Applications. London: Butterworths
- [2] Donald R. Askeland. 1994. The Science and Engineering of Materials. 3rd ed. Boston: PWS Publishing Company.
- [3] William D. Callister, Jr. 1994. Materials Science and Engineering.
- [4] Carl A. Keyser. 1986. Materials Science in Engineering
- [5] Roberts, J. 1960. High Frequency Application of Ferrites
- [6] David Jiles, 1998. Introduction to Magnetism and Magnetic Materials. 2nd ed. U.S.A.: A CRC Press Company.
- [7] By Thomas G. Reynolds. No Date. Ferrites.
- [8] Kingery, W. D., Bowen, H.K, Uhlmann D.R. 1976. Introduction to Ceramics.